JOURNAL OF CATALYSIS 149, 238–242 (1994)

# NOTE

# *In Situ* Controlled Promotion of Pt for CO Oxidation via NEMCA Using $CaF_2$ as the Solid Electrolyte

During the past 6 years, the effect of non-Faradaic electrochemical modification of catalytic activity (NEMCA) (1–9) or *in situ* controlled promotion of catalyst surfaces (10) has been described for over 25 catalytic reactions on Pt, Pd, Rh, Ag, and Ni surfaces using $O^{2-}$-conducting solid electrolytes, such as yttria-stabilized zirconia (YSZ) (2–5, 7–9), $Na^+$-conducting solid electrolytes, such as $\beta''$-$Al_2O_3$ (6, 10) and $H^+$-conducting solid electrolytes such as $CsHSO_4$ (11) as the active catalyst support. Work prior to 1992 has been reviewed (2).

In these studies, the porous catalyst film also serves as an electrode in a galvanic cell of the type

gaseous reactants, metal catalyst | solid electrolyte | metal, $O_2$

and the NEMCA effect is induced by applying currents or potentials ($-2$ to $+2$ V) between the metal catalyst and the metal counter electrode (1–11). The induced change in catalytic rate on the catalyst film can be up to $3 \times 10^5$ times higher than the rate of ion supply (2, 5) and up to 100 times higher than the catalytic rate when no voltage is applied (2, 5, 12). Significant modifications in product selectivity have also been demonstrated (2, 7). When using $\beta''$-$Al_2O_3$ as the solid electrolyte, NEMCA is due to the promoting action of spillover $Na^{\delta+}$ (1), while in the case of YSZ, NEMCA is due to the promoting action of spillover oxide ions $O^{\delta-}$ as recently confirmed by XPS (13). We report here that NEMCA can also be induced using $CaF_2$, a $F^-$ conductor (14), as the solid electrolyte.

The experimental apparatus, utilizing on-line gas chromatography, mass spectrometry (Balzers QMG 311), and IR spectroscopy (Anarad AR-500 $CO_2$ Analyzer) for continuous reactant and product analysis, has been described previously (2–10). The continuous-flow atmospheric pressure CSTR-type reactor of volume 25 $cm^3$ was of the "single-pellet" type (2, 15) (Fig. 1); i.e., the $CaF_2$ monocrystal was suspended in a quartz tube with the three electrodes, i.e., catalyst, counter, and reference, all exposed to the reactive gas mixture.

The Pt catalyst film (superficial surface area 2 $cm^2$, true surface area 80 $cm^2$, i.e., $2 \times 10^{-7}$ g-atom Pt, as measured via surface titration of oxygen with CO at 380°C (2, 3)) was deposited on the cylindrical $CaF_2$ monocrystal (diameter 2 cm, thickness 4 mm) using a thin coating of A1121 Engelhard Pt paste followed by calcination in air first at 400°C for 2 h then at 720°C for 20 min. Gold counter and reference electrodes were deposited on the other side of the $CaF_2$ disc (Fig. 1) using Demetron M8032 Au paste and the same calcination procedure as for Pt. In a series of blank experiments (no Pt), we found that the catalytic activity of the Au films for CO oxidation was less than 3% of that of Pt in the temperature range of the present investigation. In another series of blank experiments, the Pt catalyst was used as a reference electrode and no change in the rate of CO oxidation was observed upon applying currents or potentials between two Au electrodes. Consequently all the observed effects can be attributed to the catalytic properties of Pt only. Reactants were Air Liquide certified standards of 10% CO in He and 20% $O_2$ in He which could be further diluted in ultrapure He (99.995%). Constant currents $I$ between the catalyst and the counter electrode or constant potentials $V_{WR}$ between the catalyst and reference electrode were applied via an Amel 553 galvanostat–potentiostat. Due to the small currents (<1 mA) and reversed cell operation employed in the present study, $F^-$ depletion from the vicinity of the counter electrode was not a problem even after many weeks of operation.

The kinetic and NEMCA investigation was carried out using $P_{CO}$ values between 0.2 and 1.5 kPa, $P_{O_2}$ values between 3 and 10 kPa, and temperatures 500–700°C. The high operating temperatures were dictated by the very low ionic conductivity of $CaF_2$ below 500°C (14). Over this range of conditions, the rate $r$ of CO oxidation on Pt was found to conform to the phenomenological rate expression

$$r = kP_{CO}P_{O_2}^{1/2}. \quad (1)$$

The absence of external diffusional limitations was verified by varying the flowrate, and thus the velocity of impingement of reactants on the catalyst surface, and



0021-9517/94 $6.00

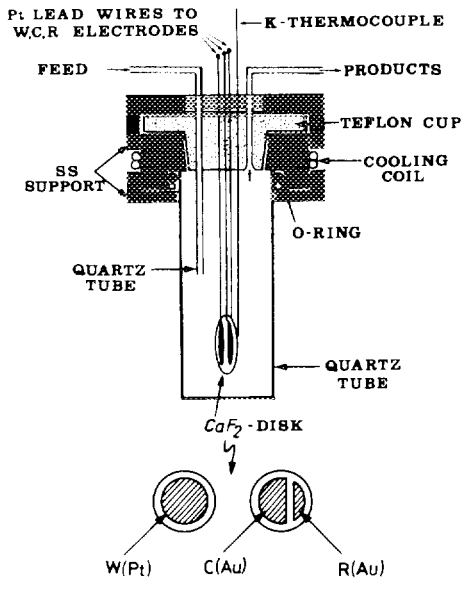


FIG. 1. Single pellet catalytic reactor and electrodes configuration.

observing no change in the measured $r$ values. The apparent rate constant $k$ was found to have a very small negative activation energy ($E_0 \approx -1$ kcal/mol). This observation, together with the observed kinetic expression (1) are consistent with the general Langmuir–Hinshelwood–Hougen–Watson (LHHW) rate expression,

$$r = k_R K_{CO} K_O P_{CO} P_{O_2}^{1/2} / (1 + K_{CO} P_{CO} + K_O P_{O_2}^{1/2})^2, \quad (2)$$

where $k_R$ is the intrinsic surface rate constant for the reaction between chemisorbed CO and O, and $K_{CO}$ and $K_O$ are the adsorption equilibrium constants of CO and oxygen, respectively. For the high temperatures of the present investigation, $K_{CO}$, $K_O$, and the surface coverages of CO and O are very small, thus Eq. (2) reduces to the experimental Eq. (1) with

$$k = k_R K_{CO} K_O, \quad E = E_R - Q_{CO} - \frac{1}{2} Q_O, \quad (3)$$

where $E_R$ is the true activation energy of the surface reaction step and $Q_{CO}$, $Q_O$ are the heats of adsorption (kcal/mol) of CO and oxygen respectively.

Figure 2 shows the effect of temperature and imposed catalyst potential $V_{WR}$ on $k$ and $E$. An interesting demonstration of the compensation effect (16) is thus obtained (Fig. 2a) with the isokinetic point ($T_\Theta$ = 800 K) lying within the temperature range of the investigation.

The observed compensation effect is a consequence of the fact that, as shown in Fig. 2b, both the apparent activation energy $E$ and the preexponential factor $k^0$, defined from

$$k = k^0 \exp(-E/RT), \quad (4)$$

increase linearly with increasing $V_{WR}$ and thus (1, 2) catalyst work function $e\Phi$. Interestingly, $r$ is also increasing with $V_{WR}$ and $e\Phi$ over the same $V_{WR}$ and $e\Phi$ range, as shown in Fig. 2a and also in Fig. 3a which depicts the effect of $V_{WR}$ on $r$ at a fixed temperature. The results of Fig. 2b can be expressed as

$$E = E_0 + \alpha_H \Delta(e\Phi), \quad (5)$$

$$k_b T_\Theta \ln(k^0/k_0^0) = \alpha_H \Delta(e\Phi), \quad (6)$$

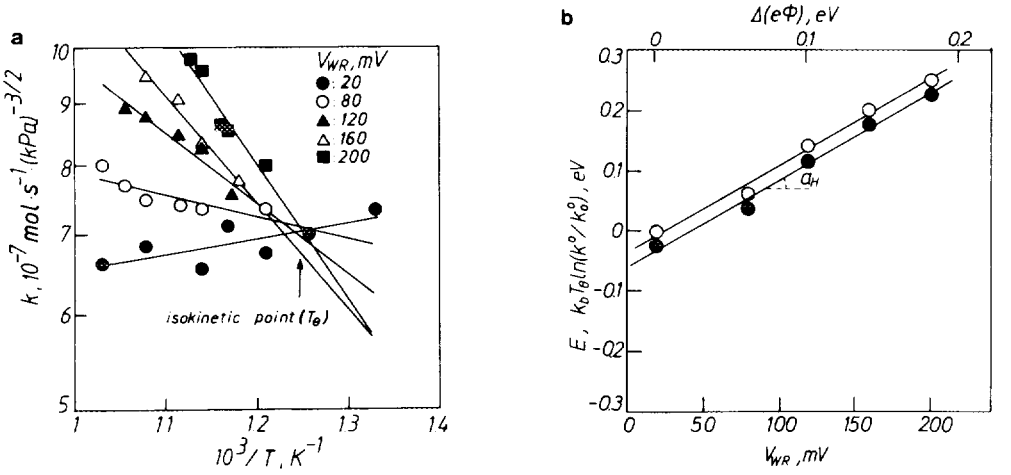


FIG. 2. (a) Arrhenius plots of the apparent kinetic constant k of the rate Eq. (1) at various fixed values of catalyst potential $V_{WR}$. (b) Effect of catalyst potential on the activation energy (filled symbols) and preexponential factor (open symbols) of the apparent kinetic constant of the reaction. The difference between closed and open symbols equals the open-circuit activation energy $E_0$ (Eqs. (5) and (6)). Conditions: $P_{O_2}$ = 6.3 kPa and $P_{CO}$ = 0.55 kPa.

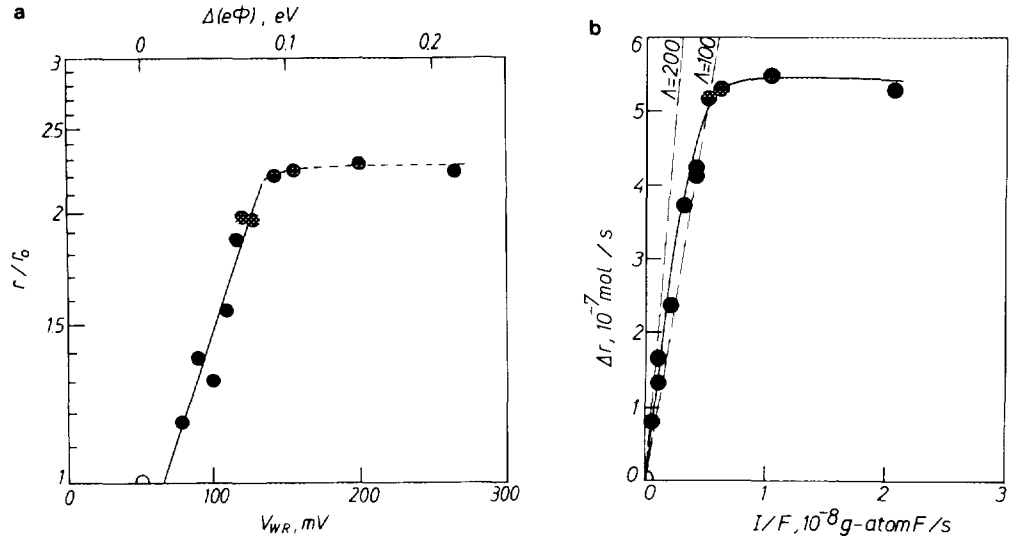


FIG. 3. Effect of catalyst potential $V_{WR}$, corresponding work function change $\Delta(e\Phi)$ (a) and corresponding applied current $I$ (b) on the rate of CO oxidation; open symbol, open circuit. Conditions: $T$ = 695°C, $P_{O_2}$ = 6.9 kPa, $P_{CO}$ = 0.4 kPa, and $r_0$ = 4.3 × $10^{-7}$ mol/s.

where $E_0$ and $k_0^0$ are the open-circuit activation energy and preexponential factor values and $\alpha_H$ = 1.45. Similar behaviour has been observed in the NEMCA studies of $C_2H_4$ oxidation on Pt/YSZ (2, 5) and on Ag/YSZ (7), and of $CH_4$ oxidation on Pt/YSZ (8). A detailed review of the NEMCA-induced compensation effect will appear elsewhere (17). In the present case, the observed increase in $E$ with increasing $e\Phi$ (Eq. (5)) can be rationalized on the basis of Eq. (4) by taking into account that increasing $e\Phi$ causes a decrease in the binding strength of electron-acceptor adsorbates such as chemisorbed oxygen and CO (2).

As shown in Fig. 3a for fixed $T$, the catalytic rate $r$ increases exponentially with $V_{WR}$ and catalyst work function $e\Phi$, over a rather narrow (~0.1 eV) $e\Phi$ range, according to the usual equation obtained in previous NEMCA studies,

$$\ln(r/r_0) = \alpha\Delta(e\Phi)/k_bT, \tag{7}$$

where the NEMCA coefficient $\alpha$ equals 0.95. Figure 3b shows the same data depicted in Fig. 3a in terms of the corresponding applied current $I$. The enhancement factor or Faradaic efficiency $\Lambda$ defined from

$$\Lambda = \Delta r/(I/F), \tag{8}$$

takes values of the order 100–200; i.e. the observed effect is clearly non-Faradaic. In a separate set of experiments at $T$ = 695°C we examined the dependence of $I$ on catalyst overpotential. The results were found to be weakly dependent on gaseous composition and to conform to the Tafel equation (2, 5, 7):

$$\ln(I/I_0) = \alpha_a F\Delta V_{WR}/k_bT, \tag{9}$$

giving the values $I_0$ = 2 × $10^{-4}$ A and $\alpha_a$ = 1 for the exchange current $I_0$ and anodic transfer coefficient $\alpha_a$. Consequently the measured $\Lambda$ values are in excellent agreement with those predicted (~200) by the following approximate expression derived elsewhere (2),

$$|\Lambda| \approx nFr_0/I_0, \tag{10}$$

where n(= 1) is the absolute value of the doping ion charge. This expression has been found to provide a good qualitative prediction of the absolute value of $\Lambda$ in NEMCA studies utilizing $O^{2-}$ conducting solid electrolytes (2).

Figure 4 shows a typical galvanostatic transient, i.e., it depicts the transient effect of a constant applied current on the rate of CO oxidation and on catalyst potential $V_{WR}$. At the start of the experiment ($t \leq 0$) the circuit is open ($I$ = 0) and the steady state catalytic rate value $r_0$ is 4.3 × $10^{-7}$ mol CO/s. The corresponding turnover frequency (TOF), based on the reactive oxygen catalyst uptake at 380°C ($N_0$ = 2 × $10^{-7}$ g-atom Pt), is 2.1 $s^{-1}$. At $t$ = 0, the galvanostat is used to apply a constant current $I$ = 300 $\mu$A between the catalyst and the counter electrode. According to Faraday's Law, fluorine ions $F^-$ are now supplied to the catalyst at a rate $G_{F^-} = I/F$ = 3.1 × $10^{-9}$ g-atom F/s. This causes an 87% increase in

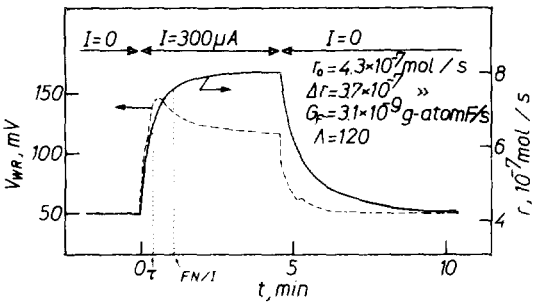


FIG. 4. Rate and catalyst potential response to step changes in applied current; $I$ = 300 μA. Conditions: $T$ = 695°C, $P_{O_2}$ = 6.9 kPa, and $P_{CO}$ = 0.4 kPa.

catalytic rate ($\Delta r = 3.72 \times 10^{-7}$ mol/s, $\rho = r/r_0 = 1.87$). The rate increase $\Delta r$ is 120 times larger than the rate $G_{F^-}$ of $F^-$ supply ($\Lambda = 120$). This implies that each $F^-$ supplied to the catalyst causes at steady state 120 chemisorbed pairs of CO and O to react and form $CO_2$.

As shown on Fig. 4, the rate relaxation time constant $\tau$, defined as the time required for the rate increase $\Delta r$ to reach 63% of its final steady-state value (2), is in excellent agreement with $FN/I$ = 64 s; $FN/I$ represent the time required to form a monolayer of fluorine on the Pt catalyst surface ($N = 2 \times 10^{-7}$ g-atom Pt) when $F^-$ is supplied at a rate $I/F$. This excellent agreement between $\tau$ and $FN/I$ provides direct evidence that the observed NEMCA behaviour is due to spillover of $F^-$ ions from the $CaF_2$ solid electrolyte onto the Pt catalyst surface,

$$F^-(CaF_2) \rightarrow F(Pt) + e^-, \qquad (11)$$

where F(Pt) stands for fluorine adsorbed on the Pt catalyst surface.

The catalyst potential and work function ($\Delta e\Phi = e\Delta V_{WR}$ (1, 2)) transient depicted on Fig. 4 shows that $\Delta e\Phi$ goes through a maximum and then approaches a steady-state value which is higher by 70 meV than the initial value. The observed increase in $e\Phi$ is consistent with the formation of F(Pt) on the Pt surface. The fact that $V_{WR}$ and $e\Phi$ go though a maximum provides strong evidence that F(Pt) is also being consumed by a surface reaction. This is also clearly demonstrated by the fact that upon current interruption (Fig. 4) both $V_{WR}$ and $r$ return to their initial steady-state value within 2–3 min. This remarkably reversible behaviour indicates that the observed non-Faradaic enhancement in the rate of CO oxidation is due to the promoting action of F(Pt). Furthermore, it shows that F(Pt) is being continuously removed from the Pt surface at a rate which is two orders of magnitude slower than the rate of CO oxidation; i.e., the TOF of F(Pt) removal is of the order of $10^{-2}$ $s^{-1}$ (Fig. 4) vs 2 $s^{-1}$ for CO oxidation.

Further investigation is required to elucidate the dominant mechanism of F(Pt) removal from the Pt surface, e.g. $F_2$ desorption, formation of $COF_2$ or $OF_2$, or eventual backmigration into the $CaF_2$ lattice. The possibility of volatile $PtF_6$ formation can be excluded because of the observed reversibility of the system and the absence of any gradual loss in catalytic activity. Regardless of the exact mechanism of F(Pt) removal, the rate transient upon current interruption (Fig. 4) conveys useful information not only about the kinetics of the F(Pt) promoter removal but also about its coverage $\theta_F$. It can be shown (17) that the $\theta_F^0$ which corresponds to a current $I$ can be computed from

$$\theta_F^0 = \frac{-(I/F)}{N} \cdot \frac{\ln(r^0/r_0)}{(d(\ln(r/r_0))/dt)_{t=t^*}}, \qquad (12)$$

where $r^0$ and $r_0$ are the rate values corresponding to $I = I$ and $I = 0$, $N$ is the catalyst surface area (g-atom Pt), and $t^*$ is the time of current interruption.

Application of Eq. (12) to the transient of Fig. 4 gives a $\theta_F^0$ value of 0.5. This in conjunction with the definition of the promotion index $P_i$ (10),

$$P_i = \frac{\Delta r/r_0}{\Delta \theta_i}, \qquad (13)$$

gives $P_i$ values of the order of 2.

The present results show that $F^-$-conducting solid electrolytes, such as $CaF_2$, can also be used to induce NEMCA via electrochemically controlled spillover of fluorine on the Pt surface. There are several similarities with the case of $O^{2-}$-conducting solid electrolytes (1–10); e.g., the reaction exhibits electrophobic behaviour for positive currents and the rate increases exponentially with $e\Phi$. The magnitude of the effect is, however, significantly smaller than in the case of $O^{2-}$-conducting solid electrolytes.

## ACKNOWLEDGMENT

We thank the CEC JOULE Programme for financial support.

## REFERENCES

1. Vayenas, C. G., Bebelis, S., and Ladas, S., *Nature (London)* **343** (6259), 625 (1990).
2. Vayenas, C. G., Bebelis, S., Yentekakis, I.V., and Lintz, H.-G., "Non-Faradaic Electrochemical Modification of Catalytic Activity: A Status Report." Catalysis Today, Vol. 11, No. 3, p. 303. Elsevier, Amsterdam, 1992.
3. Yentekakis, I. V., and Vayenas, C. G., *J. Catal.* **111,** 170 (1988).
4. Vayenas, C. G., Bebelis, S., and Neophytides, S., *J. Phys. Chem.* **92,** 5083 (1988).
5. Bebelis, S., and Vayenas, C. G., *J. Catal.* **118,** 125 (1989).

6. Vayenas, C. G., Bebelis, S., and Despotopoulou, M., *J. Catal.* **128,** 415 (1991).
7. Bebelis, S., and Vayenas, C. G., *J. Catal.* **138,** 570 (1992); **138,** 588 (1992).
8. Tsiakaras, P., and Vayenas, C. G., *J. Catal.* **140,** 53 (1993).
9. Cavalca, C., Larsen, G., Vayenas, C. G., and Haller, L., *J. Phys. Chem.* **97,** 6115 (1993).
10. Yentekakis, I. V., Moggridge, G., Vayenas, C. G., and Lambert, R. M., *J. Catal.* **146,** 292 (1994).
11. Politova, T. I., Sobyanin, V. A., and Belyaev, V. D., *React. Kinet. Catal. Lett.* **41,** 321 (1990).
12. Pliangos, C., Yentekakis, I. V., Verykios, X. E., and Vayenas, C. G., submitted for publication.
13. Ladas, S., Kennou, S., Bebelis, S., and Vayenas, C. G., *J. Phys. Chem.* **97,** 8845 (1993).
14. Rickert, H., *Angew. Chem. Int. Ed. Engl.* **17,** 37 (1978).
15. Yentekakis, I. V., and Bebelis, S., *J. Catal.* **137,** 278 (1992).
16. Schwab, G.-M., *J. Catal.* **84,** (1983).
17. Yentekakis, I. V. and Vayenas, C. G., in preparation.

I. V. Yentekakis
C. G. Vayenas

*Department of Chemical Engineering and ICEHTP*
*University of Patras*
*Patras GR-26500*
*Greece*

Received November 10, 1993; revised May 19, 1994